Hybrid Meta-Surface to Radio Telecommunication

Md. Mehedi Hasan[1*], Mohammad Rashed Iqbal Faruque[1], Mohammad Tariqul Islam[2]

[1]Space Science Centre (ANGKASA), Universiti Kebangsaan Malaysia, Bangi 43600, Malaysia
[2]Department of Electrical, Electronic and Systems Engineering, Universiti Kebangsaan Malaysia, Bangi 43600, Malaysia
mehedi20.kuet@gmail.com, rashed@ukm.edu.my, tariqul@ukm.edu.my

Abstract: Meta-surfaces offer an alternative to bulk three dimensional metamaterials. In this paper, we have pointed a 2.15 GHz wide bandwidth meta-surface for C-band applications, which is consisted of ring resonators and the size of a single unit cell is 11×11 mm^2 and the effective medium ratio is 5.27. Commercial available CST Microwave Studio electromagnetic simulator tool is used to design and numerical analysis. The numerical and the experimental results are around overlapped together. The measured transmittance (S_{21}) shows the resonance in 5.17 GHz, whereas the simulated resonance in 5.26 GHz. Besides, the proposed design is explained by the equivalent lumped element circuit model and exhibits left handed characteristics from 6.35 to 7.72 GHz in the microwave frequency range.

Keywords: C-band, Left-handed characteristics, Meta-surface.

1. Introduction

Electromagnetic meta-surfaces are artificial material with more compact size compare with conventional structures and have some infrequent properties, which does not exist in nature materials. Due to these unique properties, like negative refractive index, negative permeability, chirality, and so on. This artificial material has been received great attention in the physics and engineering communities. At presents, meta-surface is used several potential applications such as, absorption, antenna performance enhances, invisible cloaking, energy harvesting, SAR reduction, filter application, etc. EM-meta-surface were first visionary speculated by the Russian Physicist Victor Veselago in 1967. Later after a long time, in 2000, Smith and his colleagues introduced a material that shown simultaneously negative permittivity and permeability with some exceptional characteristics in microwave frequency range by combined the finite section of the negative permeability material with a negative permittivity material [1]. Further, a metamaterial was developed by capacitor loaded strips and split ring resonators in 2003 by R. W. Ziolkowski, which exhibited negative permittivity and negative permeability both at the X-band frequencies [2]. At present, for the rapid growth of the modern telecommunication systems the demand of high performances, larger bandwidth, sharp current distribution, and multi band resonance, compact in size has been increased exponentially. A compact z-shaped double negative metamaterial was exhibited for dual band application [3]. The dimension of the designed DNG metamaterial was 10 mm ×10 mm and effective medium ratio was 4.0. In 2016, a square split z-shape meta-atom with left handed characteristics, wide bandwidth was presented for S-, C-, X- and Ku-band application [4]. The presented meta-atom was investigated at 150, 300, 450, 600, 750 and 900 rotational angle. In addition, the meta-atom shown effective medium ratio 9.10 and left handed characteristics in 8.50 GHz. Further, a hybrid metamaterial was designed

by using two spiral type metamaterial patterns, which had the negative and zero permeability on a double layered PCB. The designed hybrid metamaterial had the negative and zero permeability were respectively, at the edge and the center of the metamaterial structure. Besides, the HMMs increased the power efficiency by 21.4% at 20 cm distance in 6.78 MHz [5]. A helicity multiplexed meta-surface was demonstrated by in 2015 [6]. In 2017, Hasan et *al.* projected a negative index meta-atom, resonance at C-, X- and Ku-band with wide NRI bandwidth from 7.0 to 12.81 GHz [7]. In [8] a meta-atom was reported that sensor based on planar hexagon split ring resonators to operate in terahertz frequency band. In addition, a modified version of split ring resonator was simulated for sensing dielectric changes by placing thin dielectric layers as sample materials on the full frontal surface of the sensor. In [9] a robust nature inspired optimization technique had been discussed for evolving optimal design for soft, hard and balanced meta-surfaces that would be used as broadband low-loss liners in anisotropic and dispersive boundary mode horn antennas. A hybrid graphene-gold meta-surface on SiO2/pSi/PDMS substrate presented in [10]. An optically controlled reconfigurable hybrid metamaterial that consisted of a two dimensional gold cut wire array deposited on top of a dielectric slab waveguide had been suggested for the terahertz frequencies in [11]. A hybrid structures was introduced that developed by graphene plasmonic resonators for sensing, photo-detection and nonlinear frequency generation applications by optical interactions [12].

In this paper, a hybrid and miniaturized meta-surface that is composed by the combination of two split ring resonator with metal strips in the inner ring resonator is presented. The designed meta-surface is investigated for the radio communication, since the structure is applicable for C-band application. For the experimental validation a periodic array of unit cell is fabricated and measured. The measured transmittance shows the resonance in 5.17 GHz, whereas the simulated resonance in 5.26 GHz. Due to effective medium ratio 5.80, the proposed meta-surface is compact in size and potential for practical radio telecommunication application. Further, the effect on resonance frequency by different types of substrate materials is also investigated in this paper. The paper is oriented as follows, meta-surface design methodology with the procedure of revival effective medium parameters are explained in section 2, lumped circuit model of equivalent circuit for designed meta-surface describes in section 3, section 4 shown the analysis of the results, and the paper is concluded by section 5.

2. Design of the Meta-Surface and Methodology

The proposed meta-surface structure is composed by combining the two ring resonator with an arrangement of splits and metal strips in the inner ring resonator. All the design, simulations and investigation are obtained through the computer simulation technology Microwave Studio electromagnetic simulator tool. A 1.60-mm thick (t) FR-4 substrate (dielectric constant of 4.50 and tangent loss of 0.002) is used as the host medium, while a single unit-cell dimensions are set to 11 mm, 11 mm, and 0.035 mm along the respective (x,y,z) axes. The structure is excited by a uniform plane wave propagating toward the z-direction, with its electric and magnetic fields are polarized respectively along the x- and y-axis (shown in figure 2(a)). Moreover, table 1 shows the design specification of the

proposed meta-surface single unit cell structure, where the substrate material length, width and height are respectively, ‘a’, ‘b’, and ‘t’. The metallic strips width (d) and height (h) are 0.50 mm and 0.035 mm. the splits (s) and the length and width of the inner and outer ring resonators are respectively, ‘l1’, ‘w1’, ‘l’ and ‘w’. However, figure 1 shows the schematics view, fabricated view of proposed meta-surface single unit cell and array structure.

Table 1: Configurations of the meta-surface single unit cell.

Parameters	a	b	l	w	l1	w1
Dimensions (mm)	11	11	10	9.0	8.0	7.0
Parameters	d	s	m	n	l2	r2
Dimensions (mm)	0.5	0.25	4.0	1.2	3.0	1.0

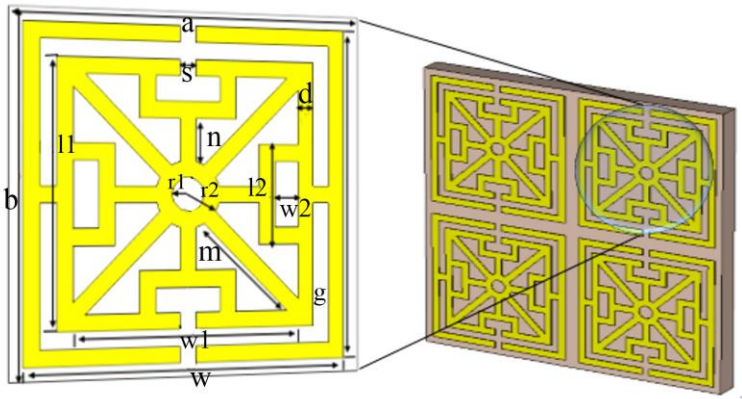

(a)

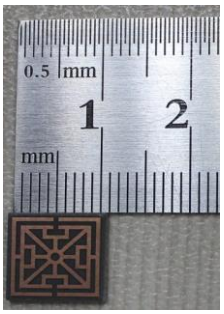

(b)

(c)

Figure 1: Proposed Meta-surface: (a) Schematic structure, (b) Fabricated single unit cell structure, (c) Fabricated array structure.

The electromagnetic properties of the proposed meta-surface are characterized numerically by using finite integration technique based CST Microwave Studio package. A single unit cell is examined with appropriate boundary conditions, where perfect electric and perfect magnetic boundaries are applied along x and y planes, so that electric field is oriented along x-direction and magnetic field is oriented along y-direction shown in figure 2(a). It also indicates that unit cells are repeated in the direction of the periodicity. In addition, the EM-waves are incident on the designed meta-surface along

the z-direction. The extraction of the necessary effective parameters and the normalized characteristic impedance of the medium is achieved form equation (1-11) and continuity of the refractive index in the frequency domain is iteratively achieved [13]. However, the effective medium parameters can be extracted from,

$$\eta = \frac{1}{kd}\cos^{-1}\left[\left\{\frac{1}{2S_{21}}\left(1-S_{11}^2+S_{21}^2\right)\right\}\pm\frac{2m\pi}{kd}\right] \quad 1$$

$$Z = \pm\sqrt{\frac{\left(1+S_{11}\right)^2+S_{21}^2}{\left(1-S_{11}\right)^2+S_{21}^2}} \quad 2$$

$$S_{11} = \left\{\frac{R_1\left(1-e^{-2j\theta}\right)}{1-R_1^2e^{-2j\theta}}\right\} \quad 3$$

$$Similarly, S_{21} = \left\{\frac{e^{-2j\theta}\left(1-R_1^2\right)}{1-R_1^2e^{-2j\theta}}\right\} \quad 4$$

where, $\theta = \zeta d \text{ and } \zeta$is the propagating constant. However, T is defined as exponential transmission.

$$T = e^{-2j\theta} = \left\{\frac{S_{21}+S_{11}-R_1}{1-R_1\left(S_{21}+S_{11}\right)}\right\} \quad 5$$

$$Similarly, R_1 = \left\{\frac{T-S_{21}+S_{11}}{1-T\left(S_{21}+S_{11}\right)}\right\} \quad 6$$

$$Permittivity, \varepsilon_{eff} = \left(\frac{\eta}{Z}\right) \quad 7$$

$$Permeability, \mu_{eff} = \left(\eta\times Z\right) \quad 8$$

$$k \approx \frac{1}{jd}\times\left[\frac{\left(1-S_{21}-S_{11}\right)\left(1+R_1\right)}{1-R_1\left(S_{21}+S_{11}\right)}\right] \quad 9$$

$$k \approx \frac{2\pi f}{c}\sqrt{\varepsilon_r\mu_r} \approx k_0\sqrt{\varepsilon_r\mu_r} \quad 10$$

$$\eta_{eff} \approx \left(\frac{k}{k_0}\right) \approx \frac{2}{jkd}\left[\left\{\frac{\left(S_{21}-1\right)^2-S_{11}^2}{\left(S_{21}+1\right)^2-S_{11}^2}\right\}\right]^{1/2} \quad 11$$

3. Lumped Element Circuit Model

The increase in the number of split rings will increase the number of split gaps and metallization on the substrate; thus, an increase in the surface electric field will be observed on the split gap areas and overall surface of the unit cell. The increasing values of overall capacitance, which includes gap and surface capacitance, will reduce the operating frequency as they are inversely proportional to each other. A simple lumped element circuit can represent the analogy of the split ring resonator. The split rings form the magnetic inductance and can be considered as inductors. The capacitance is mainly formed in and around split gap areas. The split ring resonator exhibit electromagnetic resonance when the electric energy stored in capacitor; i.e., gap is in balance with the magnetic energy stored in the inductors, i.e., split rings. The changes in capacitance, *C* and inductance, *L* due to dielectric loading from bio molecule leads to a considerable shift in the frequency of resonance. Moreover, equation (12-13) is developed for calculated the resonance peaks from the total inductance and capacitance which is formed in the lumped circuit model for the proposed design meta-surface structure by follow the ref. [14]. Therefore, the total inductance of the designed structure can be determined from the equation given as follows,

$$L_T \approx \mu_0 t \left\{ \frac{(a+b+s)^2 + (m+n+d)^2}{\pi (l+w)(l_1+w_1)} + \frac{\sqrt{l_1^2 + l_2^2 + b^2}}{\sqrt{w^2 + w_1^2 + a^2}} \right\} \quad 12$$

In addition, the total capacitance can be calculated from,

$$C_T \approx \varepsilon_0 t \left[\frac{\sqrt{l^2 + l_1^2 + m^2}}{\sqrt{d^2 + s^2}} - \ln \left\{ \frac{(a+b)^2}{\pi \left(w_1^2 - m^2 - n^2 \right)} \right\} \right] \quad 13$$

where ‘d’ is the thickness of the substrate, ‘*Z*’ is the normalize impedance, ‘*k*’ is the wave vector, ‘R_1’ is the sample interface, ‘*C*’ is the velocity of light, ‘S_{11}’ is the reflection coefficient, and ‘S_{21}’ is the transmission coefficient. Besides, free-space permeability is $4\pi \times 10^{-7}$ H/m and the permittivity is 8.85×10^{-12} F/m. So, the resonance frequency would be,

$$\textit{Resonance Frequency, } f_r = \frac{1}{2\pi \sqrt{L_T C_T}} \quad 14$$

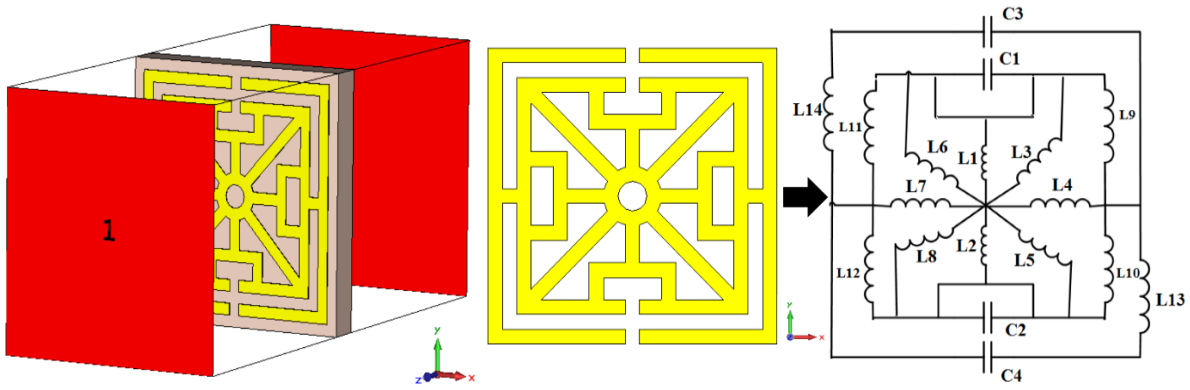

(a) (b)

Figure 2: (a) Boundary condition in simulation, and (b) Lumped equivalent circuit model of the proposed meta-surface single unit cell structure.

4. Result Analysis

The proposed meta-surface has been made of rectangular split ring resonators and arranged periodically to form of meta-surface cluster. For attaining stable magnetic and electric field response from the mentioned meta-surface based on meta-atom cluster, incidence external field has been utilized. In order to realize the transmission spectra of the meta-atom unit cell, incidence direction is horizontal to the meta-atom unit cell surface plane. When the long edges of the structure are parallel to the electric field polarization, electric response has been induced with the incident waves. When a loop is existed in the split ring resonators structure, for inducing the magnetic response, the parallel incident waves are comfortable. From the surface current distribution, it is realized that the lumped resonance is very stable and the electric field is a dominant figure on the inner ring and the outer ring with capacitive gap area indicated in figure 3(b-c). The concentration of the surface current is around the split gap due to having raised capacitance. The current flows entirely the meta-surface including the split gap area in figure 3(a).

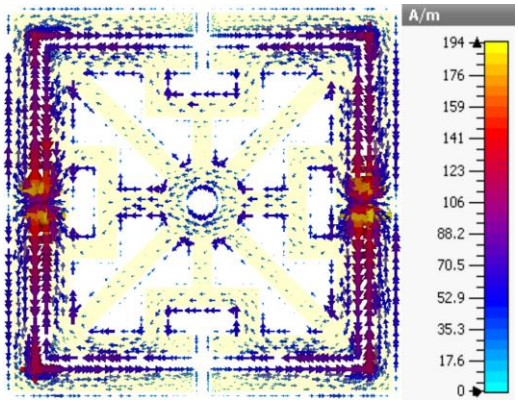

(a)

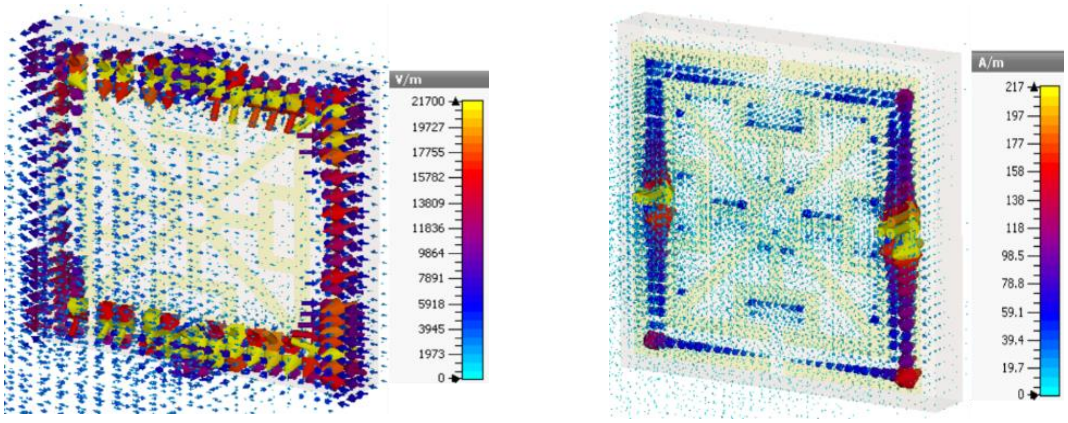

(b) (c)

Figure 3: (a) Surface current distribution, (b) Electric field, and (c) Magnetic field of the proposed hybrid meta surface unit cell at 5.26 GHz.

In order to demonstrate the performance of the meta-surface, the proposed structure is measured and the measured and the simulated results are well matched together shown in figure 4. The measured transmittance shows the resonance in 5.17 GHz, which is in the C-band and the amplitude of the resonance point, is 26.0 dB. In addition, the simulation results of the transmittance (S_{21}) is also shown in the figure 4, where the resonance point in 5.26 GHz and the magnitude of the resonance point is 43.0 dB.

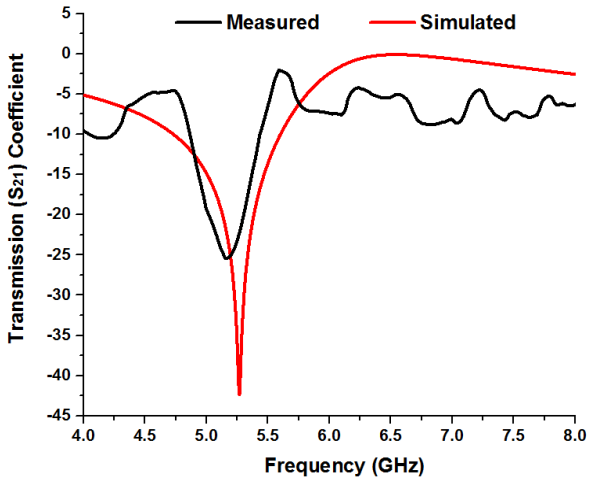

Figure 4: Measured and simulated transmittance of the proposed meta-surface.

The surface (reactance) impedance and the effective permittivity, permeability, refractive index of the designed meta-surface is exhibited in figure 5(a-d). From figure 5(a) the impedance at 5.81 GHz is (-58.44-99.0j). The permittivity curve shows two negative frequency ranges. The first one is from 4.0 to 5.44 GHz, while the second one is from 6.35 to 8.0 GHz. Further, the permeability displays negative regime from 5.86 to 8.0 GHz. which covers around 2.14 GHz. Moreover, negative refractive index is achieved at two frequency ranges, where the first one is from 4.0 to 5.22 GHz and the last one is from 5.57 to 7.72 GHz, shown in figure 5(b-d). However, the effective permittivity, permeability and refractive index curves show real magnitude of negative value from

6.35 to 7.72 GHz. According to the left handed characteristics, if the permittivity and permeability are simultaneously negative, then the refractive index will be negative. As a result, the designed structure can be called as a left handed meta-surface for any frequency points in the microwave frequency range from 6.35 to 7.72 GHz. Such as, in 6.43 GHz the real magnitude of the effective permittivity, permeability and refractive index are respectively, -68.27, -42.01, and -54.67.

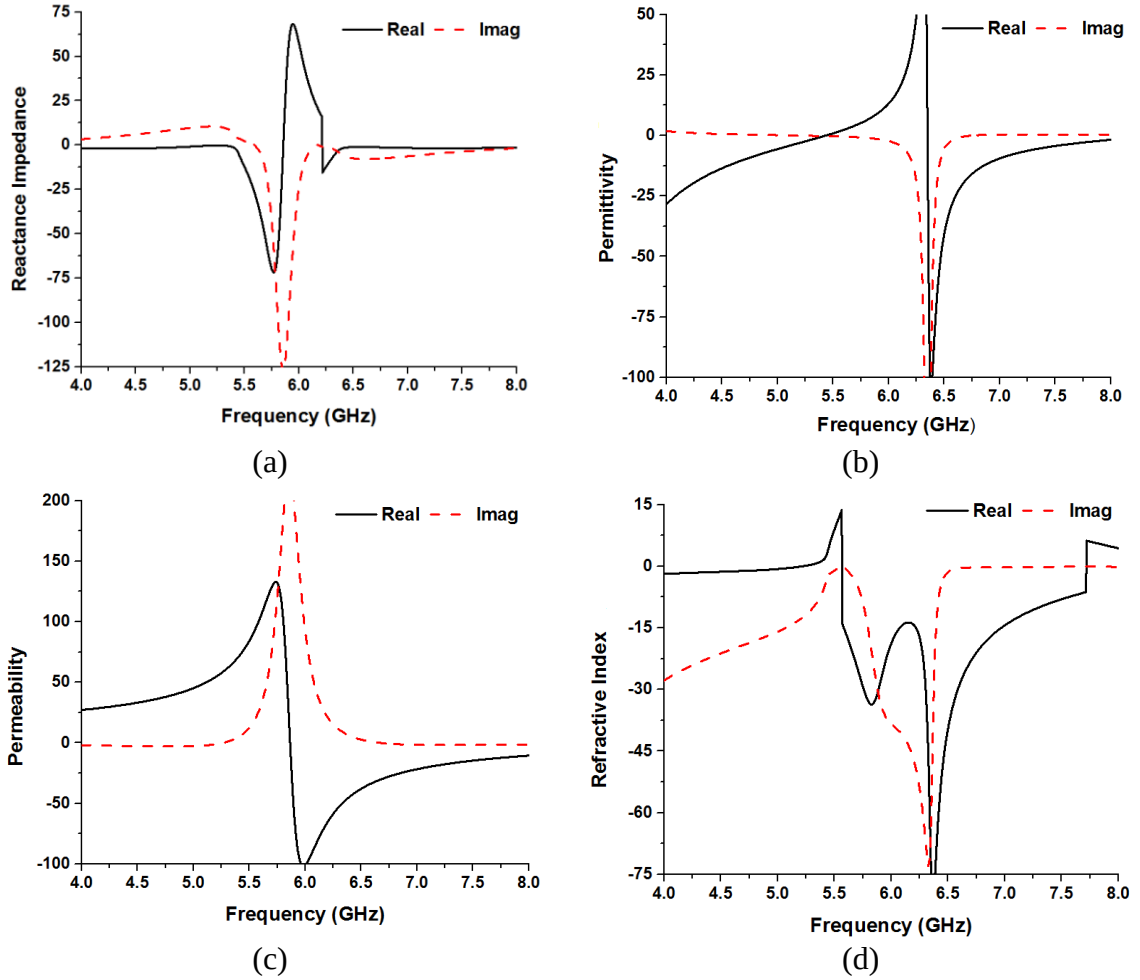

Figure 5: Amplitude of the proposed meta-surface, (a) Reactance impedance, (b) Permittivity, (c) Permeability, (d) Refractive index.

Figure 6 represents the effect on the resonance frequency through various types of materials by using as a substrate material. The dielectric constant of the FR-4, Rogers RT 5880, Rogers RT 5870, Rogers RT 6010, Rogers RT 4350, Rogers RT 4003, Mica, and Polyimide are respectively 4.50, 2.20, 2.35, 10.70, 3.66, 3.55, 5.70, and 3.50. Besides, the tangent loss of the above materials is respectively, 0.002, 0.0009, 0.0012, 0.0023, 0.0037, 0.0027, 0.0, and 0.008. If the dielectric constant is increased, then substrate material conductivity is decreased. The permittivity of a material depends on the material internal structure. When the EM-waves are propagated through a material, then the electric and magnetic fields are oscillating as sinusoidal pattern and the velocity of the atoms depend upon the conductivity, whither the conductivity depends on the internal structure. In addition, the internal pattern, permittivity, polarization, etc. caused the variation in the

results of the reflection (S_{11}) and transmission (S_{21}) coefficients. Table 2, show the dielectric constant and loss of tangent of different substrate materials.

Table 2: Dielectric materials for the proposed sample analysis.

Substrate Material	Permeability	Permittivity	Loss Tangent	Resonance in (S_{21})
Rogers RT 5880	1.0	2.20	0.0009	5.26
Rogers RT 5870	1.0	2.35	0.0012	5.17
Polyimide	1.0	3.50	0.008	4.48
Rogers RT 4003	1.0	3.55	0.0027	4.45
Rogers RT 4350	1.0	3.66	0.0037	4.40
FR-4	1.0	4.50	0.002	4.15
Mica	1.0	5.70	0.0	4.02
Rogers RT 6010	1.0	10.70	0.0023	>4.0

The transmittance resonance depends on the permittivity of the substrate material. If the permittivity is increased, then the resonance peaks are shifted toward the lower frequency. From figure 6(a-b), with the resonance peaks are sifted towards the lower frequency with the use of larger value of permittivity material used as substrate of the proposed structure. Moreover, from figure 6(b) and table 2, the resonance peaks of the substrate material are respectively, 5.26 GHz (magnitude of -42.34 dB), 5.17 GHz (magnitude of -41.95 dB), 4.48 GHz (magnitude of -40.19 dB), 4.45 GHz (magnitude of -40.28 dB), 4.40 GHz (magnitude of -38.88 dB), 4.15 GHz (magnitude of -28.46 dB), 4.02 GHz (magnitude of -6.02 dB), and less than 4.0 GHz for sequentially Rogers RT 5880 (permittivity of 2.20), Rogers RT 5870 (permittivity of 2.35), Polyimide (permittivity of 3.50), Rogers RT 4003 (permittivity of 3.55), Rogers RT 4350 (permittivity of 3.66), Epoxy Resin Fibre (FR-4) (permittivity of 4.50), Mica (permittivity of 5.70), and Rogers RT 6010 (permittivity of 10.70). The shift of the resonance frequency can be explained by the overall capacitance changes of the resonator. Increasing the dielectric constant causes an increase for each capacitance values between the ground plane and resonator.

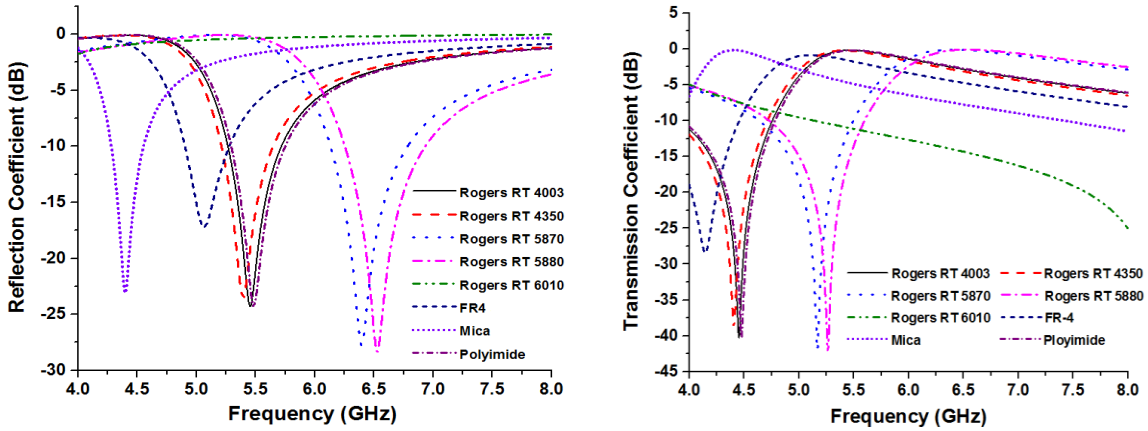

(a) (b)

Figure 6: (a) Reflection (S_{11}) coefficient, (b) Transmission (S_{21}) coefficient of the proposed meta-surface printed on different substrate material.

5. Conclusions

We have proposed a meta-surface to achieve high performance and easy to fabricate and practically applicable. The structure is composed of electric and magnetic resonators and the measured and simulated results are overlapped each other. Due to the effective medium ratio 5.80, the compact meta-surface practically applicable for C-band application. The equivalent lumped element circuit model of the proposed meta-surface is design, where the inductance and the capacitance are formed by the metal part and the splits, respectively of the proposed structure. Finally, the substrate material effects on the performance of the designed meta-surface structure is also investigated, whereas the permittivity of the substrate material is inversely proportional with the resonance peaks of the proposed meta-surface.

Acknowledgements

This work was supported by the Research Universiti Grant, Geran Universiti Penyelidikan (GUP), code: 2016-028.

References

1. D. R. Smith, W. J. Padilla, D. C. Vier, S. C. Nemat- Nasser, S. Schultz, "Composite medium with simultaneously negative permeability and permittivity", *Physical Review Letters*, 84:4184-4187, 2000.
2. R. W. Ziolkowski, "Design, fabrication, and testing of double negative metamaterials", *IEEE Transactions on Antennas and Propagation*, 51:1516–1529, 2003.
3. M. M. Hasan, M. R. I. Faruque, S. S. Islam, M. T. Islam, "A new compact double-negative miniaturized metamaterial for wideband operation", *Materials*, 9(10):830, 2016.
4. M. R. I. Faruque, M. M. Hasan, M. T. Islam, "Wideband 90^0 azimuthal miniaturized meta atom with left-handed characteristics", *IEEE Antennas and Wireless Propagation Letters*, 2016, DOI: 10.1109/LAWP.2016.2624757.
5. Y. Cho, S. Lee, S. Jeong, H. Kim, C. Songl, K. Yoon, J. Song, S. Kong, Y. Yun, J. Kim, "Hybrid metamaterial with zero and negative permeability to enhance efficiency in wireless power transfer system", *IEEE Wireless Power Transfer Conference*, 2016, Doi: 10.1109/WPT.2016.7498808.
6. D. Wen, F. Yue, G. Li, G. Zheng, K. Chan, S. Chen, M. Chen, K. F. Li, W. H. Wong, X. Chen., "Helicity multiplexed broadband metasurface holograms", *Nature Communication*, No. 8241, 2015.
7. M. M. Hasan, M. R. I. Faruque, M. T. Islam, "A Single Layer Negative Index Meta Atom at Microwave Frequencies", Microwave and Optical Technology Letters, 59:1450–1454.
8. N. Naeem, A. Ismail, A. R. H. Alhawari, M. A. Mahdi, "Terahertz dielectric sensor based on novel hexagon meta-atom cluster", *ACES Journal*, 30:9, 2015.
9. Q. Wu, C. P. Scarborough, D. H. Werner, E. Lier, X. Wang, "Design synthesis of metasurfaces for broadband hybrid-mode horn antennas with enhanced radiation

pattern and polarization characteristics", *IEEE Transactions on Antennas and Propagation*, 60:3594-3604, 2012.

10. Y. T. Zhao, B. Wu, B. J. Huang, Q. Cheng, "Switchable broadband terahertz absorber/reflector enabled by hybrid graphene-gold metasurface" *Optics Express*, 25:7161-7169, 2017.
11. X. Zhao, L. Zhu, C. Yuan, J. Yao, "Reconfigurable hybrid metamaterial waveguide system at terahertz regime", 24:18244-18251, 2016.
12. P. Q. Liu1, I. J. Luxmoore, S. A. Mikhailov, N. A. Savostianova, F. Valmorra, J. Faist, G. R. Nash, "Highly tunable hybrid metamaterials employing split-ring resonators strongly coupled to graphene surface plasmons*", Nature Communications*, 6:1-7, 2015.
13. M. M. Hasan, M. R. I. Faruque1, M. T. Islam, "Multiband left handed biaxial meta atom at microwave frequency", *Materials Research Express*, 4: 035015, 2017.
14. M. M. Hasan, M. R. I. Faruque1, M. T. Islam, "Left-handed metamaterial using Z-shaped SRR for multiband application by azimuthal angular rotations", *Materials Research Express*, Vol. 4, Number. 4, 2017.